Thermochimica Acta 477 (2008) 7–15

Contents lists available at ScienceDirect

Thermochimica Acta

journal homepage: www.elsevier.com/locate/tca

Thermodynamic analysis of a novel ammonia–water trilateral Rankine cycle

Calin Zamfirescu, Ibrahim Dincer*

Faculty of Engineering and Applied Science, University of Ontario Institute of Technology, 2000 Simcoe Street North, Oshawa, ON L1H 7K4, Canada

ARTICLE INFO

Article history:
Received 25 April 2008
Received in revised form 29 July 2008
Accepted 4 August 2008
Available online 12 August 2008

Keywords:
Ammonia–water
Trilateral flash Rankine cycle
Kalina cycle
Power generation
Performance
Efficiency

ABSTRACT

In this paper we thermodynamically assess the performance of an ammonia–water Rankine cycle that uses no boiler, but rather the saturated liquid is flashed by a positive displacement expander (e.g., reciprocating, centrifugal, rotating vane, screw or scroll type expander) for power generation. This cycle has no pinch point and thus the exergy of the heat source can be better used by matching the temperature profiles of the hot and the working fluids in the benefit of performance improvement. The second feature comes from the use of the ammonia–water mixture that offers further opportunity to better match the temperature profiles at the sink level. The influence of the expander efficiency, ammonia concentration and the coolant flow rate is investigated and reported for a case study. The optimized cycle is then compared to four organic Rankine cycles and a Kalina-type cycle and shows the best performance. It is also shown that, in order to determine the best cycle configuration and parameters, energy efficiency must be used only in conjunction with the amount of the heat recovered from the source. The efficiency of the cycle running with ammonia–water is 0.30 in contrast to steam-only case showing 0.23 exergy efficiency, which means an increment of 7.0% is obtained for the same operating conditions. If cogeneration is used the cycle effectiveness may even be over 70%. The cycle can be applied for low power/low temperature heat recovery from geothermal sources, ocean thermal energy conversion, solar energy or process waste heat, etc.

© 2008 Elsevier B.V. All rights reserved.

1. Introduction

In the past two decades some extensive efforts have been devoted to the development of thermodynamic cycles able to recover and convert into work low grade (temperature) heat sources such as waste from industrial processes, hot exhaust gases from gas turbines generators, geothermal sources, solar energy, heat rejected by topping Rankine cycles or nuclear reactors, ocean thermal energy, etc.

What is important in such applications is to match the temperature profiles at sink and source such that the available exergy could be exploited at maximum in the benefit of an improved system performance.

Using a mixture like ammonia–water is attractive in this context because of the opportunity to adjust the temperature variation during liquid–vapor phase change by regulating the ammonia concentration in the proper way. Thus it is possible to match the temperature profiles of the fluids that exchange heat at sink or source level. This is a way to minimize the destroyed exergy in the heat exchangers.

The ammonia–water Rankine cycle is in general known as Kalina cycle after the name of its inventor [1]. When designing, optimizing or modeling this kind of cycle the exergy analysis is crucial. Exergy analysis is now a mature methodology that accounts for the system's inefficiency in terms of exergy destruction, i.e., the degradation of the system ability to perform work with respect to its surroundings [2].

The exergy is calculated with the known formula, namely $e = h - h_0 - T_0(s - s_0)$, where h and s are the fluid specific enthalpy and entropy, respectively, and the index 0 indicates the environment reference conditions. A reference state must be defined in order to perform the exergy analysis. Throughout this paper we assumed the standard environment defined by $T_0 = 25\,^{\circ}\mathrm{C}$ and $P_0 = 1$ bar and for estimation of the enthalpy and entropy the following subroutines were used: (i) for water and steam the FluidProp software [3] which implements IF97 equation of state [4], and (ii) for ammonia–water properties the subroutines developed by [5] which are based on Ziegler and Trepp equations [6].

In the Kalina implementation the mixture is heated in three phases: initially the subcooled liquid is preheated up to the pinch point where it becomes saturated, the fluid is then boiled and its temperature further increases, and in the last phase the vapors are superheated. The superheated vapors are expanded in a turbine and then condensed in a so called distillation and condensation

* Corresponding author.
E-mail addresses: calin.zamfirescu@uoit.ca (C. Zamfirescu), ibrahim.dincer@uoit.ca (I. Dincer).

0040-6031/$ – see front matter © 2008 Elsevier B.V. All rights reserved.
doi:10.1016/j.tca.2008.08.002

Nomenclature

A	cross sectional area (m^2)
e	specific exergy (J/kg)
$\dot{E}$	exergy rate (kW)
f	friction coefficient
h	specific enthalpy (J/kg)
$\dot{m}$	mass flow rate (kg/s)
P	pressure (bar)
$\dot{Q}$	heat rate (kW)
s	specific entropy (J/kg K)
$\dot{V}$	volumetric flow rate (m^3/s)
$\dot{W}$	shaft power (kW)
$\tilde{W}$	relative blower work
x	vapor quality

Greek symbols

Δ	difference
ε	effectiveness
ζ	friction constant (Eq. (12)) (kg/m^7)
η	energy efficiency or isentropic efficiency
ξ	overall ammonia concentration
ρ	density (kg/m^3)
ψ	exergy efficiency

Subscripts

1	inlet
2	outlet
i	index
B	blower
cog	cogeneration
d	destroyed (exergy)
E	expander
L	liquid
max	maximum
opt	optimum
P	pump
s	isentropic
si	sink
so	source
TFC	trilateral flash cycle

Superscripts

$'$	saturated liquid
$''$	saturated vapor
$\sim$	dimensionless quantity

subsystem [7]. This subsystem includes an absorber, a vapor–liquid separator and a condenser.

According to Corman et al. [8] and Martson [9] a relatively high potential to recover the heat rejected from topping and intermediate Rankine cycles has been observed for the Kalina cycle. This technical option is compared to an alternative one, namely with the multi-pressure steam Rankine cycle, by Park and Sontag [10]. In multi-pressure steam Rankine the match between the fluids exchanging heat is attempted by boiling the water at multiple pressure stages. According to [10] the ammonia–water Rankine cycle is superior to the multi-pressure steam Rankine cycle with 5% in energy efficiency and 15% in exergy efficiency. Almost the same figures are also claimed by a series of papers by other authors [11,12].

However, at a closer look, that considers the operation of both steam and mixture cycles on the same operating conditions, Gajewski et al. [13] show that the energy efficiency of Kalina cycle is only 2.5% superior to triple stage steam cycle but the investment cost in Kalina cycle is 1.8 times higher, due to the complicated distillation and condensation subsystem. Moreover, if used at higher temperature, the ammonia decomposition becomes an issue. Similar points are sustained by Jonsson and Yan [14].

DiPippo [15] compares the ammonia–water cycle with the organic Rankine cycle and remarks that Kalina cycle may have a better efficiency with about 3%. Almost same figure has been also found in [16] for a 5 MW design.

Another cited application of the ammonia–water Rankine cycle is for ocean thermal energy conversion (OTEC). Using a warm seawater of 28 °C and cold seawater of 4 °C, Uehara and Ikegami [17] obtained 5% energy efficiency which means 62% of the Carnot cycle efficiency in the specified conditions. There are several other applications of the Kalina cycle using heat recovery such as geothermal, agricultural and industrial [18–21].

However, we note that most of the published studies on this topic concern theoretical analyses and parametric studies. There are only few known experimental implementations of the cycle up to date. The first claimed plant tested is by Leibowitz and Mirolli [22] and was built at the DOE location in Los Angeles. A second implementation has been made in Husavik, Iceland, and uses a brine temperature of 120 °C at inlet and 80 °C at outlet [23,24]. There are some pilot plant trials in Japan by the group of Amano et al. [25,26] which developed a ternary cycle using a gas turbine at the topping cycle, a steam Rankine cycle at the intermediate stage and an ammonia–water cycle at the bottoming stage. The source temperature at the bottoming stage is 165–185 °C. It was experimentally shown that there is an optimal ammonia concentration for better performance which varies in the range of 0.4–0.7.

It should be mentioned that there are some technologies that compete with the Kalina's implementation of the ammonia–water cycle in an attempt to better match the temperatures at sink and source for performance maximization.

One alternative is the supercritical steam cycle [27]. In this approach water is pumped to supercritical pressures, i.e., over ~220 bar and then heated to supercritical temperatures, i.e., over 400 °C. A perfect match between water and flue-gas can be obtained in the benefit of high cycle efficiency. However, the high pressures associated to this implementation, make it suitable for medium to high power applications (tens of MW and more) and intermediate temperature heat sources (over 400 °C).

The main competitor of the ammonia–water Rankine cycle is perhaps the supercritical organic Rankine cycle. This technology is however in very early stages of development [28]. Both low power and low temperature applications may take advantage of this technology. Only the fluid temperature profiles at source level can be matched in a supercritical ORC working with a single component fluid.

If instead of a single component organic fluid a non-azeotropic organic mixture, or the ammonia–water mixture is used, it is then possible to match both the temperature profiles at sink and source. In this assumed alternative it remains to find a suitable fluid combination that shows a reasonably critical pressure such that the technical implementation becomes economically attractive.

An interesting compromise approach, which is in fact the basis for the system presented in this paper, has been proposed by Smith et al. [29] and called the "trilateral flash cycle". In their study, R134a is used as the working fluid and is expanded in a screw expander right after the preheating. Here, the saturated liquid is flashed into two phase, the resulted vapor–liquid mixture is then fully condensed and the liquid is pumped to high pressures and heated up to the saturation temperature.

This cycle is attractive for two reasons: it matches the temperature profiles at source in a perfect manner, and it operates at reasonable pressures such that its implementation is economically feasible for low-power applications.

In this paper we propose to use the ammonia–water mixture in a novel trilateral Rankine flash cycle and investigate the opportunity to match both the temperatures at sink and source levels with the aim of overall system performance maximization. In the first part of the paper the trilateral ammonia–water flash Rankine cycle is introduced and then its modeling presented. A parametric study is subsequently performed and cycle optimization results are reported. The performance-related advantages of the proposed cycle are confirmed through comparisons with respect to other cycles.

2. The present cycle

The diagram of the ammonia water Rankine cycle that we propose is presented in Fig. 1. The cycle comprises four elements corresponding to four processes, namely a pump, two heat exchangers (resorber and liquid heater) and an expander.

In the state denoted with #1 there is a saturated ammonia water solution in liquid phase. This solution is pumped at high pressure, and it results in a subcooled liquid in #2. The liquid is then heated using the heat source stream up to the moment when it reaches the saturation in state #3. The saturated liquid is flashed (expanded) in the volumetric expander that produces work at its shaft and a liquid–vapor mixture at its outlet, in state #4. In the resorber, cooling is applied to the two-phase mixture using the heat sink stream. As a consequence, a combined process of condensation and absorption occurs (resorption) that eventually results in releasing a saturated liquid in state #1.

The thermodynamic process is represented in the *T*-s diagram as illustrated in Fig. 2. Note that the cycle presented in Fig. 2 resulted from an optimization process performed for performance maximization which is discussed later in this paper.

The key element for the implementation of this cycle is the expander that performs the process #3–4. In general, two types of expansion devices exist: turbo-machines, using kinetic energy of an expanding flow to turn a shaft at elevated rpm, and positive displacement (or volumetric) machines, operating by expanding a fixed volume of fluid per one revolution. Turbines are devised to allow for free rotation; however, the free space between blades tip and the housing allows for leakage especially at high-pressure drop per stage and at low capacity of the turbine. Blade tip leakages remain approximately constant for varying turbine size [30]

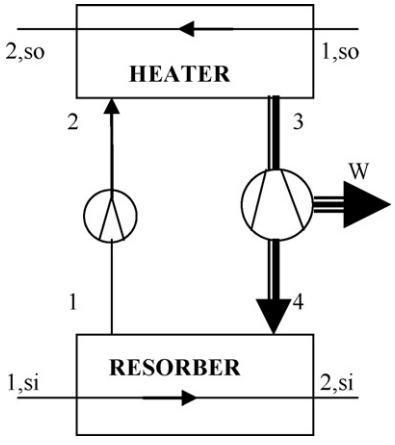

Fig. 1. The proposed ammonia–water trilateral flash Rankine cycle.

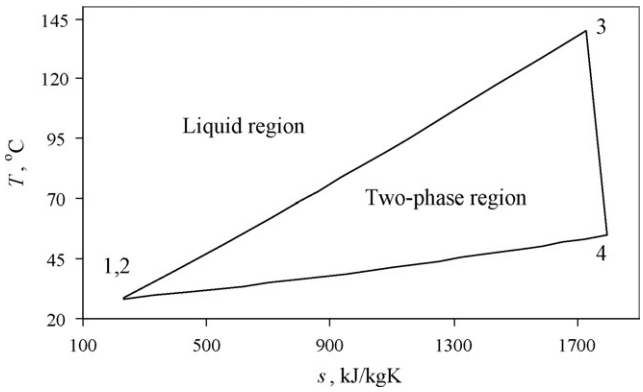

Fig. 2. The proposed cycle represented on a T-s diagram.

and therefore turbo-expanders are in principle not suitable for low power applications. There were several attempts that demonstrate that is possible and beneficial to flash liquid in refrigeration systems using positive displacement devices such as screw, scroll, reciprocating, rotating vane or turbo-machines instead of the throttling valve [31–33].

As mentioned in the introduction, Smith et al. [29] developed a power cycle similar to the one presented here, but with the difference of using a pure fluid instead of a mixture. A twin-screw type expander was employed and worked well, and its isentropic efficiency obtained in their studies reached values higher than 0.7.

The primary application of the Smith cycle has been for geothermal heat recovery. In general the geothermal brine contains impurities, particulate matter and various acids or salts. It is a common practice to flash the brine and expand the resulting (almost pure) steam in a turbine. The left liquid brine is used then either for heating purposes, or is re-injected into the well, or, in many situations it is wasted. In the cycle by Smith et al. [29], the brine is used to heat the single-component phase change fluid that runs the trilateral flash cycle.

Using screw machines for processes that evolve completely in two-phase has been also tested for ammonia–water mixture by Infante Ferreira et al. [34]. There, the screw machine was used as compressor. The liquid phase has been supplied in excess such that the need of lubrication oil has been eliminated. Since the screw machines are reversible it is quite expected that the process work efficiently the other way around, that is, in expansion mode.

A major problem with a screw expander is related to their complicated multidimensional (e.g., 3D) geometry along which the rotors mate. The mating line is relatively long and allows for large leakage flow, due to fact that the RPM of the shaft is outside the optimum range and that there is no enough liquid to seal the leakage paths. In contrast with screw expander, scroll machines have a simpler 2D geometry, and therefore, display smaller clearances and leakage paths. A scroll expander consists of two mating spiral elements assembled with 180° phase difference. During the operation, a scroll remains stationary and the other is rotated eccentrically. At the shaft of the rotating part the electrical generator is coupled. This configuration allows for the scroll to rotate in an orbiting motion within the fixed scroll. The phase difference between the two scrolls is maintained using an anti-rotation device. The relative rolling of the contact points offers less resistance than the sliding friction that characterizes the screw expanders.

Using scroll machines as expanding devices has been investigated especially for transcritical CO_2 refrigeration cycles with promising results indicating an isentropic efficiency of 50% and a volumetric efficiency of 68%, respectively [31]. Ingley et al. [30] investigated theoretically a scroll expander and concluded that

this type of expander is suitable for work production from low-temperature and low-power heat sources.

Bingchun et al. [35] studied the application of a novel adaptation of the rotary vane expander for work recovery in transcritical CO_2 refrigeration cycle. They concluded, however, that the leakages are relatively large and lead to a low volumetric efficiency. However, with extensive research and development effort rotary vane expanders are believed to be a possible choice as for work recovery in refrigeration field. Due to its similarity with many refrigerants, rotating vane expanders thus appear as a technically sound choice for ammonia–water cycles as well.

Finally one needs to mention the work by Brasz [33] where it is shown that a centrifugal compressor for the refrigerant R134a can be used as a radial inflow turbine to expand the refrigerant R245fa into two-phase for work recovery in refrigeration cycles. However, special turbine designs must be developed to obtain good efficiency, and the design is depended upon the operating conditions and the working fluid.

Regardless the type of the expander, in the parametric study conducted in this paper we assume a range of technically sound isentropic efficiency and analyze its impact on the cycle efficiency.

3. Analysis

In this section we develop a steady-state model of the proposed cycle. The energy rate balance is written for every cycle component of the system, namely pump, heater, expander and resorber, respectively, as follows:

$$\left.\begin{array}{l} \dot{W}_{\mathrm{P}} = \dot{m}(h_2 - h_1) \\ \dot{m}_{\mathrm{so}}(h_{1,\mathrm{so}} - h_{2,so}) = \dot{m}(h_3 - h_2) \\ \dot{W}_{\mathrm{E}} = \dot{m}(h_3 - h_4) \\ \dot{m}_{\mathrm{si}}(h_{2,\mathrm{si}} - h_{1,\mathrm{si}}) = \dot{m}(h_4 - h_1) \end{array}\right\} \quad (1)$$

The pump is modeled here as an isentropic process; this assumption simplifies the calculations but does not essentially affect the results. Therefore the temperature at pump discharge is calculated in function of the specified entropy and pressure; further the corresponding enthalpy is evaluated as

$$s_2 = s_1; \qquad T_2 = T(s_2, P_2, \xi); \qquad h_2 = h_L(T_2, P_2, \xi) \quad (2)$$

where the term ξ stands for the overall NH_3 concentration.

At the heater's outlet, as noted above, the liquid comes in saturated conditions. Therefore the pressure of the ammonia–water mixture is related to the temperature and concentration by the saturation condition which is written as $P_3 = P'(T_3, \xi)$.

Here, the expander works with a specified isentropic efficiency η_{E}. Thus, the actual enthalpy at discharge h_4 and temperature T_4 are calculated using the isentropic discharge enthalpy $h_{4\mathrm{s}}$.

Firstly, the state #4s corresponding to an isentropic discharge of the expander is calculated. It is therefore imposed that in state #4s the fluid has the same entropy as it has in the state #3. Then it is assumed that the discharged vapor and liquid are in thermodynamic equilibrium that is they have the same temperature and pressure. This fact allows for the estimation of the concentrations in saturated liquid ξ' and vapor ξ'' for the specified temperature and pressure using the subroutines [5].

Lastly it is written that the entropy in state #4s obeys to the mixing rule, i.e., it is a weighted sum of the entropy in liquid and vapor states. The following system of equations results therefore

$$\left.\begin{array}{l} s_{4\mathrm{s}} = s_3 \\ x_{4\mathrm{s}} = [\xi - \xi'(T_{4\mathrm{s}}, P_4)]/[\xi''(T_{4\mathrm{s}}, P_4) - \xi'(T_{4\mathrm{s}}, P_4)] \\ s_{4\mathrm{s}} = (1 - x_{4\mathrm{s}})s'(T_{4\mathrm{s}}, P_4) + x_{4\mathrm{s}}s''(T_{4\mathrm{s}}, P_4) \end{array}\right\} \quad (3)$$

The system of Eq. (3) is solved for $s_{4\mathrm{s}}$, $x_{4\mathrm{s}}$, and $T_{4\mathrm{s}}$. Then the enthalpy in #4s results with the mixing rule:

$$h_{4\mathrm{s}} = (1 - x_{4\mathrm{s}})h'(T_{4\mathrm{s}}, P_4) + x_{4\mathrm{s}}\mathrm{h}''(T_{4\mathrm{s}}, P_4) \quad (4)$$

Having the value of $h_{4\mathrm{s}}$, the actual discharge enthalpy is given by the isentropic efficiency of the expander as

$$h_4 = h_3 + (h_{4s} - h_3)\eta_E \quad (5)$$

The enthalpy and the overall concentration in the state #4 obey also the mixing rule, that is

$$\left.\begin{array}{l} h_4 = (1 - x_4)h'(T_4, P_4) + x_4h''(T_4, P_4) \\ \xi = (1 - x_4)\xi'(T_4, P_4) + x_4\xi''(T_4, P_4) \end{array}\right\} \quad (6)$$

In the conditions when all the other values are given or prior calculated, the above equations are solved for T_4 and x_4.

In many practical situations there is no water available on site to serve as coolant (or sink) for the power cycle. For this reason we consider herein that the power cycle is cooled with air from the environment, a resource which is present everywhere. Consequently, the calculation of the cycle efficiency must involve the estimation of the power consumed by the air blower. This power is taken from the expander shaft and diminishes the cycle's useful output. In order to evaluate this power we first estimate the air-flow rate at the sink heat exchanger inlet, namely $\dot{V}_{1,\mathrm{si}} = \dot{m}_{\mathrm{si}}/\rho_{1,\mathrm{si}}$. Certain air velocity corresponds to the volumetric flow rate that will generate a pressure drop:

$$\Delta P_{\mathrm{si}} = f\frac{\rho_{1,\mathrm{si}}}{2A_{\mathrm{si}}^2}\dot{V}_{1,\mathrm{si}}^2 \quad (7)$$

We observe that in the above equation the factors in front of the volumetric flow rate are always constant since $\rho_{1,\mathrm{si}}$ is evaluated at the ambient air conditions and the cross sectional area A_{si} of the heat exchanger is assumed at a fixed value. Thus, we generally estimated the pressure drop via a constant coefficient ζ that takes account for the friction losses

$$\Delta P_{\mathrm{si}} = \zeta\dot{V}_{\mathrm{si}}^2 \quad (8)$$

Based on Eqs. (7) and (8) the blower power, which is given by the product of pressure drop and volumetric flow rate, is calculated with:

$$\dot{W}_{\mathrm{B}} = \zeta\left(\frac{\dot{m}_{\mathrm{si}}}{\rho_{1,\mathrm{si}}}\right)^3 \quad (9)$$

Therefore, the useful exergy delivered by the cycle becomes:

$$\dot{W} = \dot{W}_{\mathrm{E}} - \dot{W}_{\mathrm{P}} - \dot{W}_{\mathrm{B}} \quad (10)$$

The heat delivered by the source stream and its inlet exergy are, respectively:

$$\dot{Q}_{\mathrm{so}} = \dot{m}_{\mathrm{so}}(h_{1,\mathrm{so}} - h_{2,\mathrm{so}}) \quad (11)$$

and

$$\dot{E}_{1,\mathrm{so}} = \dot{m}_{\mathrm{so}}e_{1,\mathrm{so}} \quad (12)$$

With the help of Eqs. (9)–(12) the energy and exergy efficiencies of the cycle are calculated as

$$\eta = \frac{\dot{W}}{\dot{Q}_{\mathrm{so}}} \quad (13)$$

and

$$\psi = \frac{\dot{W}}{(\dot{E}_{1,\mathrm{so}} + \dot{E}_{1,\mathrm{si}})} \quad (14)$$

In this approach, the blower is considered out of the system boundary. However, the exergy exchange between the system and the

Table 1
The fixed parameters assumed for the case study

Parameter	Value
$T_{1,so}$	150 °C
P_{so}	6 bar
$\Delta T_{1,so} = T_{1,so} - T_3$	10 °C
$\Delta T_{2,so} = T_{2,so} - T_2$	10 °C
$\Delta T_{2,si} = T_4 - T_{2,si}$	10 °C
$\dot{m}_{so}$	1 kg/s
ζ	5 kg/m^7

Table 2
The quantities varied for the parametric study

Parameter	Range
ξ	0–1
ΔT_{si} (°C)	10–40
η_E	0.6–0.8

blower is accounted for by the shaft work and the pressure increase produced by the blower. Note that the exergy at sink inlet $\dot{E}_{1,si} = \dot{m}_{si} e_{1,si}$ is slightly higher than zero, because the static pressure in the air–stream at the blower discharge is larger than the environment pressure. In the calculations reported in the next section, a value of 2 kPa has been assumed for the overpressure produced by the blower for all studied cases; this value is technically sound for the scale of the application from our case study.

A second approach to study exergy efficiency further is included in the next section according to Eq. (19), where the blower is included within the system's boundary and thus the exergy of the air–stream is not considered at all.

In the next section the mathematical model of the cycle, as described by the Eqs. (1)–(16), is exploited to study the influence of the important design parameters and to find their optimal values that maximize the cycle performance.

4. Results and discussion

We consider here a case study which refers to a geothermal energy conversion case similar to the one published in Ref. [36] where the liquid brine is available at a temperature of about 150 °C. Here, we conduct a parametric study aiming at the maximization of the cycle efficiency. To this respect we fix the number of parameters to constant values, as listed in Table 1. These values were chosen based on engineering data specific to the case study. The water inlet temperature corresponds to the one from the case study [36] and the water pressure is chosen such that no boiling can occur; the temperature differences listed in Table 1 refer to the minimum temperature differences at the heat exchangers; the mass-flow rate of source flow is chosen unity for simplicity; the pressure drop coefficient is estimated at an average value according to the considerations discussed in the previous section. In principle, what is demonstrated herein will work for other set of fixed parameters.

For calculation of the air enthalpy we assumed that the air components are oxygen, nitrogen and argon with molar concentrations of 0.205, 0.79, and 0.05, respectively, and used FluidProp software [3] for enthalpy and density evaluation. In addition, we consider that the brine enthalpy can be evaluated with the equation of state IF 97 [3,4], which is specific to pure water.

The parametric study is conducted with respect to three parameters, namely the overall ammonia concentration, the temperature variation at sink, and the isentropic efficiency of the expander. Their considered range of variation is listed in Table 2.

A calculation scheme has been elaborated that solves the balance Eq. (1) together with the additional Eqs. (2)–(14) for the fixed parameters listed in Table 1 and particular values of the three variables listed in Table 2.

The first results refer to the variation of the exergy and energy efficiencies with the overall ammonia concentration for a fixed value of the isentropic efficiency of the expander, $\eta_E = 0.7$. These results are presented graphically in Fig. 3(a) and (b) for energy and exergy efficiency, respectively.

As it can be observed from these results, there is an optimal ammonia concentration that maximizes the exergy efficiency. Its value depends on the assumed temperature glide of the coolant (at the sink level). The meaning of the coolant's temperature glide should be understood in correlation to the coolant mass flow rate. Namely, a large mass flow rate means a small temperature glide, but in the same time a high power consumed by the blower.

The small temperature glide at coolant side leads however to lower temperatures in the resorber, and therefore to higher power output at the expander shaft. It has to be recalled that in our parametric study we assumed a fixed temperature difference between the coolant and the working fluid at the sink outlet (see Table 2 for $\Delta T_{2,si}$). There is a limit of reduction of ΔT_{si} after which $\Delta T_{2,si}$ cannot be maintained to the desired value and it must be reduced too. This limit has been 18 °C for our input data.

Regarding the energy efficiency, the same trend is observed as for the exergy efficiency, with the only difference that the optimal values of ammonia concentration ξ for which the maximum efficiency is obtained are slightly larger than those corresponding to exergy efficiency maximization.

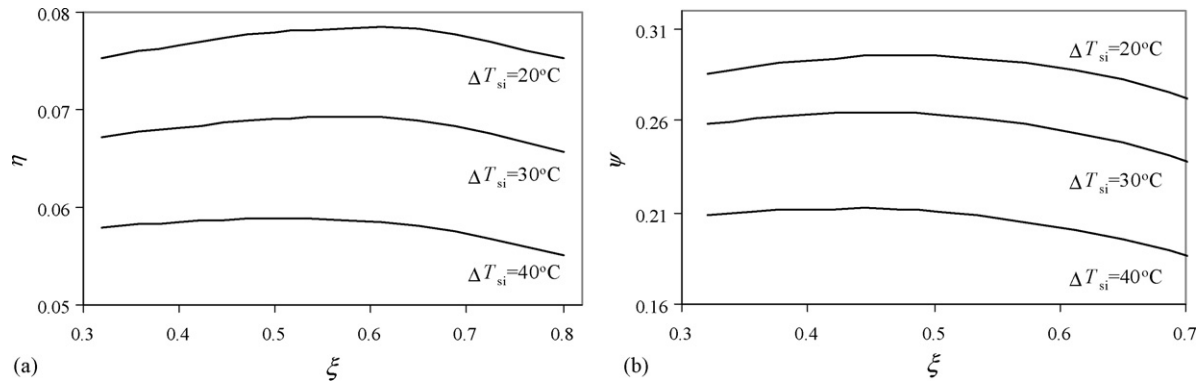

Fig. 3. The influence of the overall ammonia concentration on the cycle efficiency for a fixed $\eta_E = 0.7$ and three fixed values of the coolant temperature glide. (a) Energy efficiency and (b) exergy efficiency.

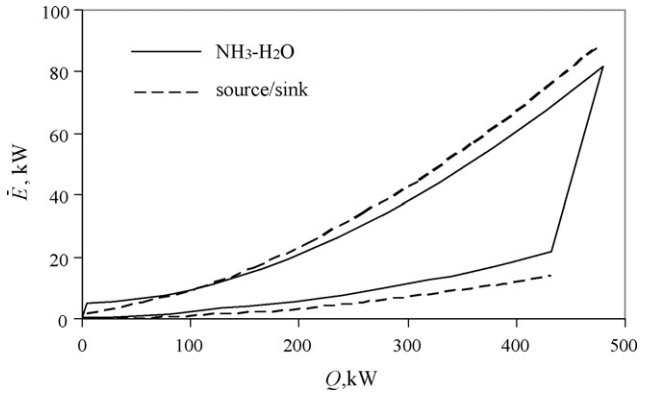

Fig. 4. The $\dot{E} - \dot{Q}$ diagram for the cycle with maximum exergy efficiency $\eta_E = 0.7$, $\Delta T_{snk} = 20\,^{\circ}C$, $\xi_{opt} = 0.47$, $\varepsilon_{max} = 0.42$ and $\eta = 0.08$.

In Fig. 4, it is illustrated the thermodynamic cycle in the $\dot{E} - \dot{Q}$ diagram. In order to form this diagram, the flow enthalpy in the state 1, has been set to zero, that is the point $(\dot{Q}, \dot{E})_1 = (0, \dot{E}_1)$ in the diagram. Then we calculate them for the ammonia–water mixture:

$$(\dot{Q}, \dot{E})_i = (\dot{Q}_{i-1} + \dot{m}(h_i - h_{i-1}), \dot{E}_i), \quad i = 1, 2, 3, 4, 5, \ldots\ldots \tag{15}$$

For the source we set $\dot{Q}_{2,so} = \dot{Q}_2$ and

$$(\dot{Q}, \dot{E})_{1,so} = (\dot{Q}_{2,so} - \dot{m}_{so}(h_{2,so} - h_{1,so}),\ \dot{m}_{so}e_{1,so}) \tag{16}$$

and for the coolant side we set $\dot{Q}_{1,si} = 0\,kW$ and

$$(\dot{Q}, \dot{E})_{2,si} = (\dot{Q}_{1,si} + \dot{m}_{si}(h_{2,si} - h_{1,si}),\ \dot{m}_{si}e_{2,si}) \tag{17}$$

Our next point in the study is to analyze the impact of the expander isentropic efficiency on the cycle efficiency. This study has been performed for a fixed temperature glide at sink, $\Delta T_{si} = 2\,^{\circ}C$, and the results are reported in Fig. 5 in the form of energy efficiency (a) and exergy efficiency (b) as a function of the ammonia concentration for three values of the expander's isentropic efficiency.

Practically, the optimal ammonia concentration that can be observed in the curves plotted in Fig. 5 is not influenced by the magnitude of the expander efficiency. The expander efficiency influences in a linear way the exergy and the energy efficiency, respectively.

Here, we now include the co-generation option when the warm air discharged by the blower is used for some heating purposes. Therefore, we introduce the cogeneration cycle effectiveness as

$$\varepsilon_{cog} = \frac{\dot{W} + \dot{E}_{2,si}}{\dot{E}_{1,so} + \dot{E}_{1,si}} \tag{18}$$

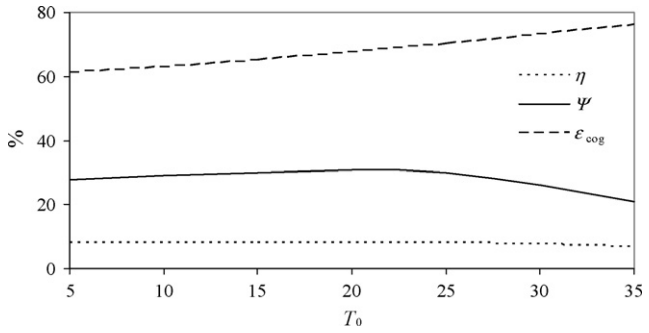

Fig. 6. The energy and exergy efficiencies and the cogeneration effectiveness as a function of the dead state temperature, for a fixed discharge air temperature at sink, $T_{2,si} = 45\,^{\circ}C$ and $\eta_E = 0.7$.

where the exergy of the hot air stream represents an output of the cycle.

The cycle cogeneration effectiveness depends also upon the reference environment (dead state) temperature. Such dependence is clearly presented in Fig. 6 for a constant air temperature at sink outlet. In the same graph we also present the variation of exergy and energy efficiencies. As it can be remarked, for the range of dead state temperature assumed in the analysis, the energy efficiency is practically constant (it slightly changes with T_0, for example 8–7%). However, the exergy efficiency changes drastically with T_0 as presents a maximum at $T_0 = 20\,^{\circ}C$, and the cogeneration effectiveness increases with T_0.

Here we now discuss the advantages of the proposed trilateral ammonia–water flash cycle with respect to other implementations of the Rankine cycle. In order to make a fair comparison, this analysis is constrained to single-stage Rankine cycles. As "competitors" of the ammonia–water trilateral flash cycle we consider here four organic Rankine cycles (ORC) and one Kalina-kind cycle all operating under the same conditions at sink and source. More exactly, for all cycles the temperature (e.g., 150 °C) and the flow rate at source inlet (e.g., 1 kg/s) are the same; in other words the exergy of the source stream $\dot{E}_{1,so}$ is fixed for all cases. The isentropic efficiency of 0.7 is assumed for the expander as a kind of representative value.

For the organic Rankine cycles, we selected, based on critical temperature and pressure, four organic fluids namely R141b (1,1-dichloro-1-fluoroethane), R123 (2,2-dichloro-1,1,1-trifluoroethane), R245ca (1,1,2,2,3-pentafluoropropane), and R21 (dichlorofluoromethane). A trial and error procedure is also employed to determine the optimum pressures of the cycle that maximize its exergy efficiency for each

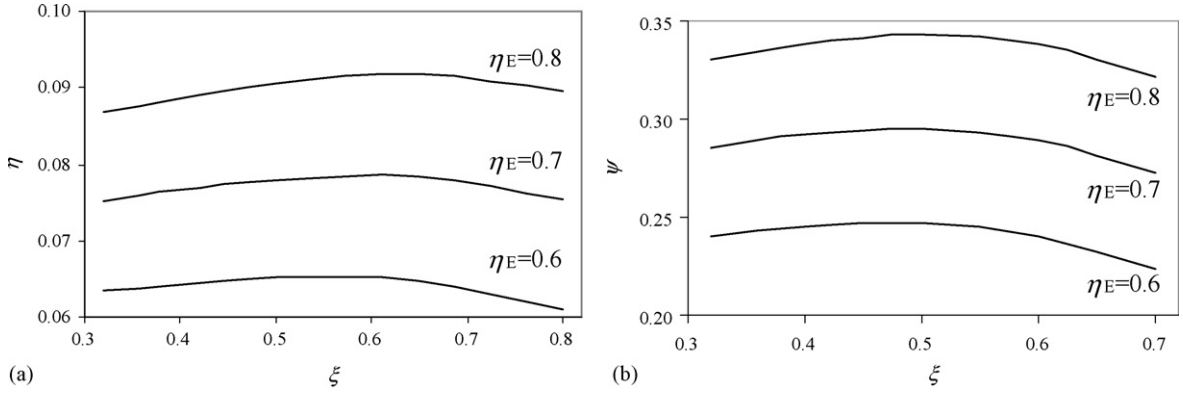

Fig. 5. The influence of the overall ammonia concentration on the cycle exergy efficiency for a fixed $\Delta T_{snk} = 20\,^{\circ}C$ and three fixed values of the expander isentropic efficiency. (a) Energy efficiency and (b) exergy efficiency.

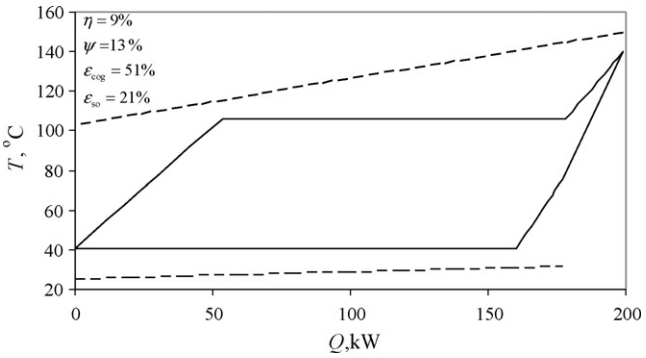

Fig. 7. The $\dot{Q} - T$ diagram of the organic Rankine cycle with R21.

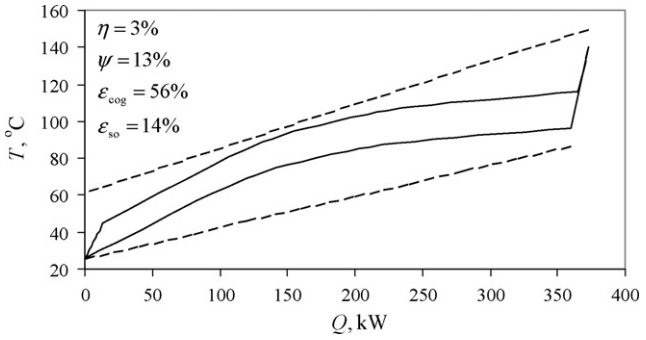

Fig. 8. Kalina-type ammonia–water cycle.

fluid. One exemplary organic Rankine cycle is illustrated in Fig. 7.

The Kalina-type cycle that we consider here is of a simplified and modified version for analysis purposes, in the way that the distillation and condensation units are replaced with a resorber. This is made in order to get a consistent comparison in terms of system complexity: that is, all the compared systems have the same number of four components. This cycle is illustrated in Fig. 8, and as it can be observed, it has rather low energy efficiency, even though the exergy efficiency is the same as that of the ORC from Fig. 7.

The results of this comparative analysis are presented in Table 3 that includes a series of relevant parameters as to be explained here. The first one is the energy efficiency as computed via Eq. (13). Surprisingly, the cycle that we propose here, denoted with "trilateral" in Table 3, features an energy efficiency of 8% as compared to the ORC–R141b that displays the highest efficiency of 10%. This is only apparently a drawback, because in our case study the cycle with maximum energy efficiency delivers the least work, as it will be shown below.

Table 3
Performance comparison among various cycles

Parameter	ORC cycles				NH_3–H_2O cycles	
	R141b	R123	R245ca	R21	Kalina	TFC
η (%)	10	9	9	9	3	8
ψ (%)	13	16	16	13	13	30
ε_{cog} (%)	27	36	40	51	56	71
$\dot{Q}_{so}$ (kW)	132	179	189	198	373	477
$\dot{W}$ (kW)	13	17	18	18	13	38
ε_{so} (%)	15	19	20	21	14	43
ε_E (%)	34	43	45	57	76	93
$\dot{E}_d$ (kW)	19	26	28	31	60	42
r_{so} (%)	34	36	36	36	62	23
r_{si} (%)	38	37	36	25	14	62
r_E (%)	27	27	27	38	24	15

The trilateral flash cycle (TFC) features, however, a two times larger exergy efficiency than all other options. Moreover, TFC cogeneration effectiveness is the highest as 71%; the second largest one is for Kalina-type cycle, and the smallest is obtained for the R141b. This demonstrates that the cycle with the highest energy efficiency recovers inefficiently the heat from the source.

In Table 3, we also show the heat rate extracted from the source in all cases for comparison purpose to demonstrate how much comes from each one. The results indicate that the R141b cycle extracts the least heat from the source as 132 kW, while the trilateral flash cycle receives the most, i.e., 3.6 times more than that as 477 kW. This is due to the fact that the TFC uses the most of the source's exergy because both the source fluid (water) and the working fluid (ammonia–water) are in liquid state and have similar specific heats, and thus the temperature difference in the heat exchanger is minimized. However, there is not the some case for any of the ORC cycles: they can recover at most ~40% (R21 case) from the amount of heat recovered by the TFC.

This reality clarifies why, from all the studied cases, the trilateral flash cycle with 8% energy efficiency delivers the maximum amount of work at the expander shaft (38 kW), as compared to 13 kW delivered by the R141b-cycle with 10% energy efficiency. In relative terms, the ability of the cycle to recover and convert the source heat into work is measured by the following quantity as

$$\varepsilon_{so} = \frac{\dot{W}}{\dot{E}_{1,so}} \tag{19}$$

that represents the overall cycle effectiveness relative to the source stream exergy. Since the source stream exergy is fixed, the cycle that converts the most of it into work (or useful exergy) is the best.

The values for ε_{so} are listed in the same Table 3 and reveal that the R141b cycle converts in fact the least of source energy into useful work (15%), and, among ORC the R245ca and R21 the most (19%). However, our proposed cycle converts the most of source exergy (43%) that is about three times more than for the cycle with maximum energy efficiency (R141b). This is due to the "construction" of the TFC, which is made such that it matches perfectly the temperature profiles at sink and source.

For example, one can analyze the cycle ability to use the source's exergy, through the following effectiveness:

$$\varepsilon_E = \frac{\dot{E}_3}{\dot{E}_{1,so}} \tag{20}$$

as the ratio between the exergy of the stream about to be expanded and that of the heat source. One observes from Table 3 that the trilateral flash cycle recovers the most of the source's exergy as 93%, the Kalina-type cycle the second most as 76% while the R141b cycle becomes the least as 34%, respectively.

The other point one should raise is that why the trilateral flash cycle does not show also the maximum energy efficiency? This is because the recovered heat from the source is large and acts as a denominator in the efficiency definition Eq. (13). In addition, the expansion in two-phase takes place across smaller enthalpy differences than expansion in gas phase (in relative terms).

In Table 3, we also included the total exergy destruction and the percentage of destruction per every component of the cycle as defined as

$$r_i = \frac{\dot{E}_{d,i}}{\dot{E}_d}, \quad i = \text{so, si, E} \tag{21}$$

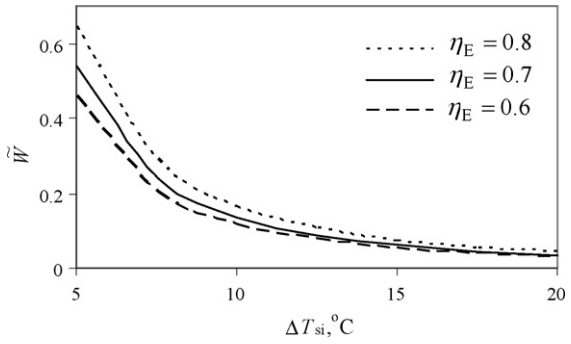

Fig. 9. The ratio between blower and expander shaft power as a function of the temperature glide at sink and η_E.

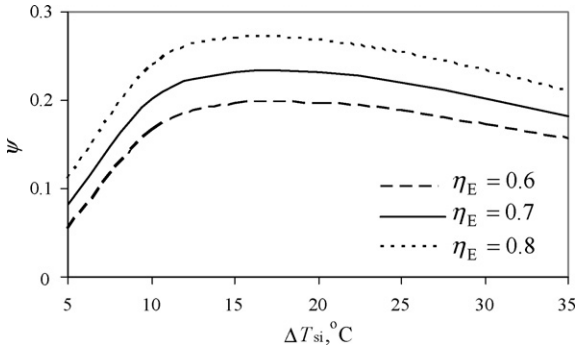

Fig. 10. The exergy efficiency of the cycle with pure water as a function of the temperature glide at sink and η_E.

For our trilateral flash cycle the most of exergy destruction take place at the level of the sink heat exchanger, showing that this is a key element for performance improvement.

It is obvious that if the source temperature is higher, both energy and exergy efficiencies of all analyzed cycles will increase. However, the trilateral flash cycle will qualitatively maintain the same properties to better match the temperatures at both source and sink and better use the source exergy content. This means that the results presented here for the case of 150 °C source temperature stand also for other values of $T_{1,so}$.

Another aspect treated in this section refers to the extreme situations when the ammonia concentration is set to zero or unity for the trilateral flash cycle. Since these two cases are qualitatively the same, we report here only on the situation when the ammonia concentration is set to zero, that is the trilateral flash cycle is run with pure water.

Note that in the particular case of a single component working fluid, the condensation process evolves at constant temperature. Because of this reason, the temperature profiles of the fluids exchanging heat at sink level cannot be well matched. This fact induces the drawback of an additional exergy destroyed, which results in lowering the cycle exergy efficiency.

The parameter that controls the coolant temperature profile is only the air-flow rate. A large air-flow rate is translated in a small temperature glide that will induce an increase of the expander shaft power. But, to maintain a large flow rate more power must be extracted from the expander's shaft to run the blower.

Fig. 9 shows the power taken by the blower from the expander shaft in function of the temperature glide at the coolant. The result is reported in a dimensionless form as the ratio between blower and expander power $\tilde{W} = \dot{W}_B/\dot{W}_E$.

In fact, the power required by the blower to maintain a small temperature glide at the sink heat exchanger increases dramatically and this induces a reverse trend in the evolution of the cycle efficiency: while the temperature glide is reduced, the cycle efficiency tends to increase first, and then it decreases. These aspects are clearly observed in Fig. 10 where it is demonstrated that the exergy efficiency has a maximum for a given temperature glide at the sink stream.

In addition, the $\dot{Q} - T$ diagram, is plotted for the pure water cycle in Fig. 11(a) and for the trilateral flash cycle in Fig. 11(b) for comparison purpose. The exergy efficiency of the steam cycle is 0.23 as compared to 0.30 for the ammonia–water case. This difference can be understood by observing the large temperature drop at the sink heat exchanger in the case of steam condensation.

Note that the steam cycle has been optimized with respect to the choice of sink flow rate (i.e., the temperature glide), and an expander performing with the same isentropic efficiency of 0.7 has been considered for the two compared cases. More precisely, the optimized steam cycle, namely the cycle displaying the maximum ε has been selected based on the results plotted in Fig. 10, from where it results that for $\eta_E = 0.7$ the optimum $\Delta T_{si} = 17$ °C, respectively.

Furthermore, there may be other cycles that may compete with the ammonia–water trilateral flash cycle presented herein. One example is the one recently proposed by Goswami and Xu [37]. In this cycle ammonia is expanded to refrigeration temperature (below the ambient), then used for cooling purpose and then absorbed in water. This cycle of cooling and power co-generation shows high efficiency, comparable to the trilateral flash cycle. However, it is a much more complex cycle comprising at least nine components in contrast to four components of the triangular flash cycle. This fact reflects in cost/performance analysis which is a major factor in renewable energy.

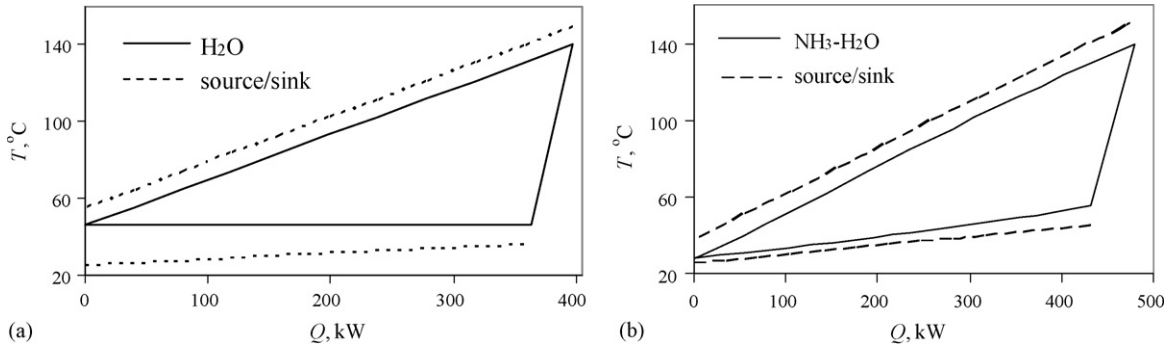

Fig. 11. Comparison of single component fluid and two-component fluid TFC in $\dot{Q} - T$ diagram. (a) Steam cycle, $\eta_E = 0.7$, $\Delta T_{si,opt} = 17$ °C, $\xi = 0$, $\psi = 23\%$ and $\eta = 8\%$ and (b) $\eta_E = 0.7$, $\xi = 0.5$, $\psi = 30\%$ and $\eta = 8\%$.

5. Conclusions

In this paper we have undertaken a study to thermodynamically assess the performance of an ammonia–water Rankine cycle with no boiler, but rather the saturated liquid is flashed by a volumetric expander (e.g., reciprocating, centrifugal, screw or scroll type expander) for power generation. Also, its performance results are compared with the ones obtained for conventional organic Rankine cycle and a Kalina-kind cycle having a resorber instead of the usual distillation and condensation subsystem. Here, we can summarize some concluding remarks as follows:

- If the flow rate and temperature of the hot source are kept constant, the maximum energy efficiency criterion can lead to an unsuitable choice of the thermodynamic cycle; rather the combination of energy efficiency and amount of recovered heat will lead to the best choice of the cycle.
- By using the non-azeotropic ammonia–water mixture the temperature profiles at both sink and source heat exchangers may be optimally adjusted for performance maximization.
- The trilateral flash cycle outperforms the considered ORC and Kalina-kind cycle because of its ability to recover most of heat from the source.
- The benefit of using the mixture with respect to single component working fluid (steam) results from the comparison of the exergy efficiency in the two cases: the mixture cycle has 0.30 and the steam cycle 0.23 exergy efficiency that is roughly 7% gain for the same operating conditions.
- The single component cycle is less efficient due to its in-ability to match the temperature profiles at sink.
- If cogeneration is used the cycle effectiveness is over 70%.
- The cycle is simple, has only four components; the key element is the expander; the expander being of positive displacement type is robust and suitable for low power applications; some problems may arise related to the material selection because ammonia–water solution is corrosive and the cavity process may occur in the expander, thus possibly damaging the metallic surface.
- The parametric study presented here constitutes a methodology that can be applied to other similar case studies on the same system.
- The model presented here may be applied for extended parametric studies and optimizations.

Acknowledgement

The authors acknowledge the support provided by the Natural Sciences and Engineering Research Council of Canada.

References

[1] A. Kalina, Journal of Engineering for Gas Turbines and Power 106 (1984) 737–742.
[2] I. Dincer, M. Rosen, Exergy, Elsevier Science, London, 2006.
[3] P. Colonna, T.P. van der Stelt, FluidProp: A Program for the Estimation of Thermo Physical Properties of Fluids, Energy Technology Section, Delft University of Technology, The Netherlands, 2004, www.FluidProp.com.
[4] W. Wagner, A. Kruse, Properties of Water and Steam: the Industrial Standard IAPWS-IF97 for the Thermodynamic Properties and Supplementary Equations for Other Properties, Springer–Verlag Berlin, Heidelberg, 1998.
[5] C. Zamfirescu, Dynamic Link Library for Ammonia–Water Thermo-Physical Properties Computation, Delft University of Technology, Engineering Thermodynamics Group, Report K301, 2001.
[6] B. Zigler, Ch. Trepp, International Journal of Refrigeration 7 (1984) 101–106.
[7] C.H. Marston, Mechanical Engineering 114 (1992) 76–81.
[8] J.C. Corman, R.W. Bjorge, A. Kalina, MPS Review (1995) 19–22.
[9] C.H. Marston, Journal of Engineering for Gas Turbines and Power 112 (1990) 107–116.
[10] Y.M. Park, R.E. Sontag, International Journal of Energy Research 14 (1990) 153–162.
[11] A. Kalina, Utility-scale combined-cycle power system with kalina bottoming cycles. Advanced power systems, Transactions of the American Nuclear Society 54 (4) (1987) 1–4, paper #5581286.
[12] C.H. Marston, M. Hyre, Gas turbine bottoming cycles: triple pressure steam versus Kalina, Transaction of the ASME 117 (1995) 10–15.
[13] W. Gajewski, A. Lezuo, R. Nürenberg, B. Rukes, H. Vesper, VGB Kraftwerkstechnik 69 (5) (1989) 411–417.
[14] M. Jonsson, J. Yan, Gas turbine with Kalina bottoming cycle versus evaporative gas turbine cycle, in: Proceedings of the 2001 International Joint Power Generation Conference, New Orleans, June 4–7, 2001, pp. 77–85.
[15] R. DiPippo, Geothermics 33 (2004) 565–586.
[16] A. Kalina, H. Leibowitz, Geothermal Resources Council Transactions 13 (1989) 605–610.
[17] H. Uehara, Y. Ikegami, Parametric performance analysis of OTEC using Kalina cycle, in: Joint Solar Engineering Conference, ASME, 1993, pp. 203–207.
[18] A. Kalina, Geothermal Resources Council Transactions 30 (2006) 747–750.
[19] H. Mlcak, Geothermal Resources Council Transactions 26 (2002)707–713.
[20] C. Koroneos, D. Rovas, Electricity from geothermal energy with the Kalina cycle—an exergy approach, International Conference on Clean Electrical Power (2007) 423–428.
[21] R. Gordon Bloomquist, Geothermics 32 (2003) 475–485.
[22] H. Leibowitz, M. Mirolli, Power Engineering (1997) 44–48.
[23] R. Maack, P. Vladimarsson, VDI-Berichte 1703 (2002) 107–116.
[24] D. Johnson, H. Mlcak, Geothermal Resources Council Transactions 26 (2002) 731–734.
[25] Y. Amano, T. Hashizume, K. Takeshita, M. Akiba, Y. Tanzawa, Experimental results of an ammonia–water mixture turbine system, in: Proceedings of the 2001 International Joint Power Generation Conference, New Orleans, June 4–7, 2001, pp. 69–75.
[26] K. Takeshita, Y. Amano, T. Hashizume, Experimental results on an ammonia–water mixture turbine system (part 2: effect of the ammonia mass fraction), in: Proceedings of the 2002 International Joint Power generation Conference, Phoenix, AZ, June 24–26, 2002, pp. 959–964.
[27] G. Tsiklauri, R. Talbert, B. Schmitt, G. Filippov, R. Bogoyavlensky, E. Grishanin, Nuclear Engineering and Design 235 (2005) 1651–1664.
[28] J.E. Boretz, Supercritical organic Rankine engines, in: Proceedings of the 21st Intersociety Energy Conversion Engineering Conference: Advancing toward Technology Breakout in Energy Conversion, San Diego, CA, USA, 1986, pp. 2050–2054.
[29] I.K. Smith, N. Stosic, C.A. Aldis, Development of the trilateral flash cycle system. Part 3. The design of high efficiency two-phase screw expanders, Proceedings of the Institution of Mechanical Engineeers, Part A 210 (A2) (1996) 75–93.
[30] H.A. Ingley, R. Reed, D.Y. Goswami, Optimization of a scroll expander applied to an ammonia/water combined cycle system for hydrogen production, in: Proceedings of the Solar World Congress, Orlando, FL, August 2–12, 2005, Paper 1545.
[31] H.J. Huff, R. Radermacher, M. Praissner, Experimental investigation of a scroll expander in a carbon dioxide air-conditioning system, in: Proceedings of the International Congress of Refrigeration 2003, Washington, D.C., 2003, Paper 485.
[32] J.J. Brasz, V. Shistla, N. Stosic, I.K. Smith, Development of a twin-screw expressor as a throttle valve replacement for water cooled chillers, in: Proceedings of the 15th International Compressor Conference, Purdue, July, 2000, http://www.staff.city.ac.uk/∼sj376/biblio.htm.
[33] J.J. Brasz, Transforming a centrifugal compressor into a radial inflow turbine, in: Proceedings of the International Compressor Engineering Conference, Purdue, July 12–15, 2004, Paper C060.
[34] C.A. Infante Ferreira, C. Zamfirescu, D. Zaytsev, International Journal of Refrigeration 29 (4) (2006) 556–565.
[35] Y. Bingchun, Z. Hansong, G. Bei, H. Zhilong, P. Xueyuan, X. Ziwen, Development of rotary vane expander for CO2 trans-critical refrigeration cycle. Seventh IIR Gustav Lorenzen Confernece on Natural Working Fluids, Trodheim, Norway, May 28–31, 2006, 1–8.
[36] H.K. Ozturk, O. Atalay, A. Yilanci, A. Hepbasli, Energy Sources Part A: Recovery Utilization and Environmental Effects 28 (2006) 1415–1424.
[37] D.Y. Goswami, F. Xu, ASME Journal of Solar Energy Engineering 121 (1999) 91–97.